CFD ANALYSIS ON QUADCOPTER

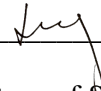**by**

LIANG JIA XIONG

Thesis submitted in fulfilment of the requirements for the

Bachelor Degree of Engineering (Honours) (Aerospace Engineering)

JULY 2024

ENDORSEMENT

I, (Liang Jia Xiong) hereby declare that all corrections and comments made by the supervisor and examiner have been taken into consideration and rectified accordingly.

_____
(Signature of Student)

Date: 23 July 2024

_____
(Signature of Supervisor)

Name: Prof Dr Farzad Ismail

Date: 23 July 2024

_____
(Signature of Examiner)

Name: Dr Chang Wei Shyang

Date: 23 July 2024

DECLARATION

This thesis is the result of my own investigation, except where otherwise stated and has not previously been accepted in substance for any degree and is not being concurrently submitted in candidature for any other degree.

————————————————————————

(Signature of Student)

Date: 9-7-2024

ABSTRACT

This thesis investigates the impact of varying the velocity inlet angles on the aerodynamic performance of the quadcopter. This study encompasses a range of inlet angles from 0° to 40° at rotational speed of 3000 rpm utilizing a multi-faceted approach that combines computational fluid dynamics simulations, quantitative performance metrics and thrust coefficient analysis. The pressure contour visualization and vorticity visualization reveal significant changes in aerodynamic characteristics as the inlet angles increase. Thrust coefficient analysis further highlights the critical role of airflow, showing stable performance in static conditions but a marked efficiency declination of from 0° to 40° under dynamic airflow conditions. The study identifies an optimal operational range between 0° and 20° inlet angle, balancing lift and thrust. This comprehensive analysis contributes to the advancement of the quadcopter technology enabling more informed design decisions and operational strategies for a greater performance across diverse flight conditions

ABSTRAK

Tesis ini mengkaji kesan perubahan sudut aliran masuk halaju terhadap prestasi aerodinamik quadcopter. Kajian ini merangkumi pelbagai sudut aliran masuk dari 0° hingga 40° pada kelajuan putaran 3000 rpm menggunakan pendekatan pelbagai faset yang menggabungkan simulasi dinamik bendalir komputasi, metrik prestasi kuantitatif dan analisis pekali tujah. Visualisasi kontur tekanan mendedahkan perubahan ketara dalam ciri-ciri aerodinamik apabila sudut aliran masuk meningkat. Analisis pekali tujah seterusnya menekankan peranan kritikal aliran udara, menunjukkan prestasi yang stabil dalam keadaan statik tetapi penurunan kecekapan yang ketara dari 0° hingga 40° dalam keadaan aliran udara dinamik. Kajian ini mengenal pasti julat operasi optimum antara sudut aliran masuk 0° dan 20°, mengimbangi daya angkat dan tujah. Analisis komprehensif ini menyumbang kepada kemajuan teknologi quadcopter, membolehkan keputusan reka bentuk dan strategi operasi yang lebih bermaklumat untuk prestasi yang lebih baik dalam pelbagai keadaan penerbangan.

ACKNOWLEDGEMENTS

First and foremost, I would like to express my gratitude to my final year project supervisor, Prof Dr Farzad Ismail. His support and guidance has made this project possible. The Universiti Sains Malaysia Computational Fluid Dynamics group has also given me the opportunity to develop my presentation skills and seek for advice on problems faced throughout the project.

Without a doubt this project cannot be completed without the resources provided by the School of Aerospace Engineering USM. The Ansys Fluent software in CATIA Lab was always available throughout my period of research.

Last but not least, I wish to extend my acknowledgement to researchers working on similar topic. The foundation of the theoretical and technical aspects behind this numerical study comes from their work. It is an opportunity to study beyond the scope of university's coursework syllabus and to experience how proper research is conducted.

Table of Contents

LIST OF FIGURES

LIST OF TABLES

LIST OF SYMBOLS

η	Efficiency of the propeller	-
C_T	Thrust coefficient of the propeller	-
C_p	Power coefficient of the propeller	-
J	Advance ratio of the propeller	-
P	Power	W
T	Thrust force	N
ρ	Density	kg/m^3
n	Rotational speed	Rps
D	Diameters of the Propeller	m
ϵ	Turbulence dissipation rate	-
μ	Dynamic viscosity	kg/ms
p	pressure	Pa
M	Mach number	-
dt	Time step size	mm
m	Mesh size of rotating domain	mm

Chapter 1

INTRODUCTION

1.1   Background and Overview

Quadcopters are one of the variants of unmanned aerial vehicle (UAV), which are rapidly developing and widely adopted over the past few decades. Initially, they were primarily used for recreational purposes and hobbyist activities including aerial photography and competitive drone racing, however recently due to the advancement in technology such as the flight control systems, sensors and sort have greatly expanded their application in other industries such as military, agriculture et cetera.

The versatility of the quadcopters has led to their use in a wide range of applications. In agriculture, quadcopters are used for crop monitoring, pesticide spraying and soil analysis. In environmental monitoring, they assist in mapping terrains, tracking wildlife and accessing natural disasters. Additionally, quadcopters also used in search and rescue operations, for instance a group of quadcopters can be used to efficiently search for missing people in a dangerous area autonomously.

Despite there are many applications of the quadcopters, they are facing significant aerodynamic challenges that can affect their performance, stability, and efficiency. The aerodynamics of quadcopters are complex due to the interaction of multiple rotating propellers and their effect on the surrounding airflow. Unlike fixed-wing aircraft, which have relatively stable and predictable aerodynamic characteristics, quadcopters operate under a variety of dynamic conditions that introduce variability in aerodynamic forces.

1.2   Problem Statement

Quadcopters have gained significant traction across various industries due to their versatility, agility and ease of deployment. Despite their widespread applications, the aerodynamic performance of quadcopters still remain an area filled with challenges especially at the interaction between the propellers and the surrounding airflow. Traditional aerodynamic studies have predominantly focused on hover and steady forward flight conditions however in real life scenarios, quadcopters have been frequently encounter with dynamic and complex airflow due to environmental factors such as wind gusts, turbulence and varying angle of attack during manoeuvres.

One critical yet underexplored aspect of quadcopter aerodynamics is the impact of different angles of the velocity inlet on the performance of the propellers. In real life, there are many accidents are due to the fluctuating cross flow causing a significant influence to the thrust and the overall stability of the quadcopters. Without a comprehensive understanding of these effects, quadcopters may have suboptimal designs leading to a less stable and reduced efficiency in corporate with the real world operating conditions.

To address this challenge, this study is to understand how different velocity inlet angles affect the aerodynamic performance of quadcopters such that engineers can optimize their design and improve its overall flight performance. It can provide insight into how the propellers generate thrust and experience drag under different conditions and additionally to develop an advanced flight control algorithms that can adapt to changing conditions ensuring a more reliable and efficient operation.

1.3   Objective of Research

The research work described in this thesis is performed to achieve the following objectives :

1. To analyse the effects of varying velocity inlet angles on the thrust of the quadcopters

2. To evaluate the impact on aerodynamic efficiency of the quadcopters.

3. To study the flow instability around the quadcopter

1.4   Scope of Research

This study is based on the numerical simulation of quadcopters under varying angles of the velocity inlet using the Ansys Fluent software. The quadcopter used in this study for the simulation is DJI Phantom 3. The propeller on the other hand is DJI Phantom 3 9450. The quadcopter will be subjected to range of velocity inlet angles to simulate different environmental conditions and flight manoeuvres. The gravitational effect is neglected to simplify the simulation.

The flow is in low speed (0.009 Mach) and the flow around the propeller is approximately at Mach number of 0.2 making it the maximum Mach number less than 0.3. This indicates that the flow throughout this study is subsonic and incompressible flow, such that there is no shockwave influence the main objectives of this study

The quadcopter subjected at $0°$ velocity inlet angle will act as the baseline of the simulation and is used to compare with the quadcopter at varying velocity inlet angles. The rotational speed is maintained at 3000 and 7000 revolutions per minute and the performance evaluation is based on the differences in thrust coefficient.

While experimental validation is not directly performed in this study, the simulation results will be compared against established experimental data from previous

studies. This comparative analysis aims to validate the accuracy and reliability of the CFD simulations in capturing real-world aerodynamic phenomena. The study also aims to provide insights into the aerodynamic performance under varying flow conditions, contributing to the understanding and optimization of quadcopter design for practical applications

1.5   Thesis Layout

This thesis comprises five main chapters : Introduction, Literature Review, Methodology, Results and Discussion, Conclusion and Recommendations. Each chapter is further divided to several sub-chapters as appropriate.

Chapter 1 focuses on the overview of this current study, the problem statement and objectives of this study. Chapter 2 is the foundation of this study, which is a review of cutting edge technology regarding this study. Chapter 3 proposes the methods and softwares employed for this investigation. The results from the investigation are presented and discussed in chapter 4. The final chapter marks the conclusion as well as recommendations for future works.

Chapter 2

LITERATURE REVIEW

This chapter aims to contextualize the current study within the broader field of aerodynamics and UAV performance analysis, highlighting the key findings and gaps in the literature.

2.1 Aerodynamics performance of Quadcopter

The main principle behind the manoeuvrability and control of quadcopters is Newton's third law and Bernoulli's principle, For instance, to make a quadcopter to throttle, every propellers will rotate in equal highspeed causing pressure difference between the top and the bottom to guarantee a steady moving up motion. [1]

The aerodynamic performance of a quadcopter is primarily determined by the lift, drag and thrust forces acting on its propellers. Lift is the upward force that opposes the weight of the quadcopter while drag is the force that opposes the motion of the quadcopter where Thrust is the forward force that drives the quadcopter forward. [2]
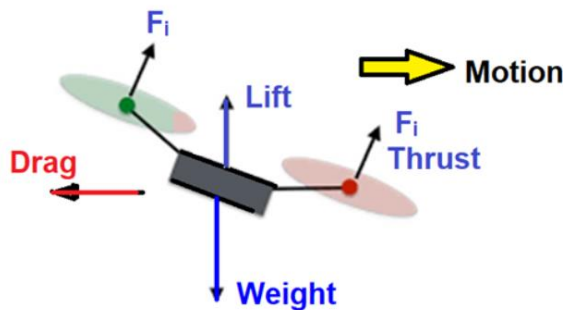
Figure 2.1: Free Body Diagram of the forces acting on the quadcopter

These propellers performance is highly dependent on the geometry of the blade, rotational speed of the blade also the incoming airspeed. To evaluate the aerodynamic performance of the quadcopter (generally the propellers), there are some analytical approaches involved including momentum-blade element theory. [3][4]

The momentum-blade element theory is a combination of momentum theory and blade element theory. With this theory, researchers had performed various modifications such as the Prandtl tip and root losses , Reynold number drag correction and sort. According to this theory, the efficiency of the propeller is expressed as follows:

$$\eta = \frac{C_T}{C_p}J \tag{2.1}$$

Where,

η = efficiency of the propeller

C_T = thrust coefficient of the propeller

C_p = power coefficient of the propeller

J = advance ratio of the propeller

From the theory, it is noticeable that the efficiency is dependent on the thrust coefficient, power coefficient and the advance ratio of the propeller.

Thrust coefficient and power coefficient of the propeller on the other hand can be expressed as follows,

$$C_T = \frac{T}{\rho n^2 D^4} \tag{2.2}$$

$$C_p = \frac{P}{\rho n^3 D^5} \qquad (2.3)$$

Where,

C_T = Thrust coefficient

C_p = Power coefficient

P = Power

T = Thrust force

ρ = density of air

n = rotational speed (revolution per second)

D = diameters of the propeller (m)

As can be seen, the aerodynamic performance of the quadcopter can be determined by the thrust coefficient and the power coefficient.

Deters, R.W and Kleinke,s [5] have done a thorough analysis on the static propulsion elements for small multirotor unmanned aerial vehicles with the objective to provide a guide for UAV researchers during propeller selection and to compare the resulting endurance. In their research, the propellers and the aircraft motors involved are shown in Table 2.1 below. For this study, the experimental data (thrust coefficient and power coefficient) of DJI Phantom3 DJI 9450 Plastic will be used for validation of our numerical results. The setup of their experiment is shown in Figure 2.2.

Table 2.1: Aircraft rotor and Propeller specification

Aircraft Motor	Propeller	Diameter (in)	Voltage (V)
3D Robotics Solo	Solo	10.0	14.8
	APC 10×4.5 MR	10.0	14.8
DJI Phantom 3	DJI 9450 Plastic	9.45	15.2
	DJI 9450 Carbon	9.45	15.2
	APC 9.5×5 MR	9.5	15.2
	Master Airscrew MR 9.4×5	9.45	15.2
	APC 9×4.5 MR	9.0	15.2
	Master Airscrew MR 9×4.5	9.05	15.2
Hubsan X4 Pro	X4 Pro	9.4	11.1
Helimax FORM500	FORM500	12.05	11.1
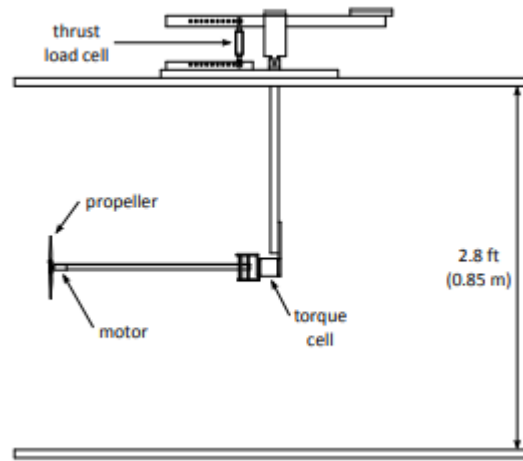
Figure 2.2: Experimental setup to evaluate the aerodynamic parameters

Several studies have been performed to use Computational Fluid Dynamics analysis as one of the common approaches for propeller aerodynamic performance. This thorough CFD analysis allow for detailed visualization and analysis of flow patterns, pressure distributions and vorticity around the propeller blades.

Penkov and D.aleksandrov [6] have studied on the effect of shrouded propeller on the lift force of unmanned quadcopter. It explored the influence of shroud parameters on the aerodynamic performance through CFD simulation and laboratory experiments. They concluded that the CFD simulation confirmed the experimental results with the propeller without shroud. They also concluded that the optimal gap between the propeller and

shroud is found to be less than 1mm for maximum efficiency but uses 3mm gap for practical implementation due to the reliability concerns. This research gives an outstanding insight into designing a propeller.
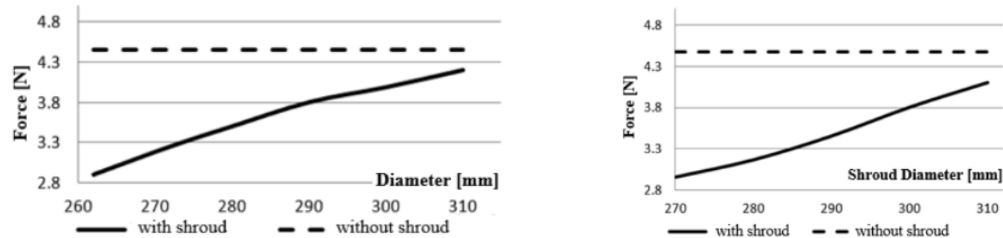
Figure 2.3: Comparative Result between Numerical Computed (left) and Experimental Results (right)

Figure 2.4: Shrouded Propeller Used in the Experiment**Error! Reference source not f ound.**

Numerical and experimental studies were conducted on an owl inspired propeller with various serrated trailing edge aimed to analyse noise reduction capabilities. This research concludes that serrated trailing edge can reduce noise level can impact vortex evolution, breaking down vortices and accelerating dissipation. This further highlights that CFD simulation are trustworthy in simulating the real world scenario which can help in design optimization.[7]

2.2   Turbulence modelling in CFD

Turbulence modelling is a critical aspect of CFD simulations as it greatly affects the accuracy of the numerical results. Various turbulence models, such as Reynolds-Averaged Navier-stokes (RANS), Large Eddy Simulation (LES) and Direct Numerical Simulation (DNS) are used depending on the complexity and the computational resources available. Normally, RANS models are used due to their computational efficiency in contrast with LES and DNS.

K-epsilon turbulence model is one of the most widely used RANS models in CFD simulation. It can solve two transport equations which is the turbulent kinetic energy (k) and one for the turbulent dissipation rate (epsilon) which can be expressed as below.[8]

Transport equation for k :

$$\rho \frac{\partial k}{\partial t} + \rho \nabla \cdot (Uk) = \nabla \cdot \left[\left(\mu + \frac{\mu_t}{\sigma_k}\right)\nabla k\right] + P_k + P_b - \rho\epsilon \qquad (2.4)$$

Transport equation for ϵ :

$$\rho \frac{\partial \epsilon}{\partial t} + \rho \nabla \cdot (U\epsilon) = \nabla \cdot \left[\left(\mu + \frac{\mu_t}{\sigma_\epsilon}\right)\nabla\epsilon\right] + C_1 \frac{\epsilon}{k}(P_k + C_3 P_b) - C_2 \rho \frac{\epsilon^2}{k} \qquad (2.5)$$

Where,

ρ= Density of the fluid

U = Mean velocity field

μ = Dynamic viscosity of the fluid

μ_t= Eddy viscosity

P_k= Production of k due to mean velocity gradients

P_b = Production of k due to buoyancy

C_1, C_2, C_3 = Model constant

Numerous studies have been conducted stating that k-epsilon model is validated for various aerodynamic applications. One of the research study the aerodynamic drone propeller at different angle of attack at different rotational speed uses k-epsilon turbulence model. It concludes that at 45° of angle of attack at the root of the propeller without twisted blade has contributes the highest thrust coefficient and gives the lowest drag coefficient.[9]

Besides that, a research conducted on a full quadcopter to analyse the condition of the quadcopter at steady wind condition. In this paper, the researcher used K-epsilon turbulence model, and they confirmed that they obtained an accurate wake structure compare with the experiment data. Ultimately, k-epsilon model is good enough to use in this simulation.

Other than using k-epsilon model, the popular options are Shear-stress transport and Spalart Allmaras. K-omega turbulence model is directly applicable to the wall in the viscous sublayer which make it suitable in low Reynold turbulence model without the need for addition damping functions. The two transport equation of k-omega can be expressed as follow. [10], [11], [12]

For k,

$$\frac{\partial}{\partial t}(\rho k) + \frac{\partial}{\partial x_i}(\rho k u_i) = \frac{\partial}{\partial x_i}\left[\Gamma_k \frac{\partial k}{\partial x_j}\right] + G_k - Y_k + S_k \qquad (2.6)$$

Where,

$\frac{\partial}{\partial t}(\rho k)$= Local time derivative of the turbulent kinetic energy multiplied by fluid density

$\frac{\partial}{\partial x_i}(\rho k u_i)$= Convective transport of k by the mean velocity field

$\frac{\partial}{\partial x_i}\left[\Gamma_k \frac{\partial k}{\partial x_j}\right]$= Diffusive transport of k

Γ_k=Effective diffusivity of k

G_k= Production of k due to mean velocity gradients

Y_k= Dissipation of k

S_k= Sinks of k

For ω,

$$\frac{\partial}{\partial}(\rho\omega) + \frac{\partial}{\partial x_i}(\rho\omega u_i) = \frac{\partial}{\partial x_i}\left[\Gamma_\omega \frac{\partial \omega}{\partial x_j}\right] + G_\omega - Y_\omega + D_\omega + S_\omega \qquad (2.7)$$

Where,

$\frac{\partial}{\partial}(\rho\omega)$= Local time derivative of the specific dissipation rate multiplied by fluid density

$\frac{\partial}{\partial x_i}(\rho\omega u_i)$= Convective transport of ω by the mean velocity field

$\frac{\partial}{\partial x_i}\left[\Gamma_\omega \frac{\partial \omega}{\partial x_j}\right]$= Diffusive transport of ω

Γ_ω=Effective diffusivity of ω

G_ω= Production of ω due to mean velocity gradients

Y_ω= Dissipation of ω

D_{ω}= Cross-diffusion term, which accounts for the interaction between k and ω

S_{ω}= Sinks of ω

Spallart allmaras equation on the other hand is an one equation turbulence model unlike the other two turbulence model mentioned. Any transportable scalar quantity can be transported using the equation expressed below. [11]

$$\frac{DF}{Dt} = \frac{\partial F}{\partial t} + (u.\nabla)F = \textit{Diffusion} + \textit{Production} - \textit{Destruction} \qquad (2.8)$$

Lopez et al.[13] has carried out CFD simulation on a quadcopter model, Araknos V2. The researcher has performed the simulation using two different turbulence models which is the k-omega SST and Spalart Allmaras turbulence model at two different rotational speed. The researcher conclude that k-omega model has predicted the torque and thrust coefficient higher than those in Spalart Allmaras model, but showing the same tendency. The biggest difference was found between the two models is the visualization of the wake.

2.3   Studies on the angle of incidence of the velocity inlet

There are many reasons for a quadcopter to fail, one of which is the bad weather conditions of the situation of quadcopter[14], [15], [16], [17]. Hence, many researchers have conducted study on the effects of these gust to the quadcopter performance.

In the study of the effect of gusty flow on aerodynamic performance of multirotor drone , the researchers have modified various propeller using Adkins and Liebeck theory for hovering flight and tested through a wind tunnel and simulations. They conclude that lower rotational speeds made the propellers more susceptible to cross flow and

fluctuating cross flow. The study also suggests that introducing three dimensional flow or separation effects in the geometry design of propeller might further improve the performance. [18]

Weerasinghe and Monasor [19] has carried out an experiment through wind tunnel and done CFD simulation on a SYMA X5SC quadrotor, focusing on the fuselage and rotor blades. Both steady and unsteady flow simulations were conducted, examining hover, forward, and side wind cases at different angles of attack and free stream velocities. In their research, CFD simulation was used to analysed the quadcopter's flow field and its performance. They had validated that the simulation results are matched in unsteady wind condition but showed inconsistencies for steady simulation. Ultimately CFD simulations effectively describe complex quadrotor flows and are reliable for analyzing flow and aerodynamic features, confirming their practical demand and utility.

Lei and Cheng [20] on the other hand had done research on the aerodynamic performance of hex rotor UAV with existing horizontal airflow (0 m/s - 4 m/s). It summarize that at high rotational speed, the incoming wind adversely affects the aerodynamic performance of the rotors.

2.4   Study the instability of quadcopter

Stability and control mechanisms are especially important to managing the dynamic forces acting on quadcopter during manoeuvring. Control systems, such as PID (Proportional-Integral-Derivative) controllers are commonly implemented to stabilize the quadcopter based on the sensor feedback. Studies have been conducted on quadcopter control using PID, and one of them is that Praveen and Pillai have developed a PID controller to enhance the stability of the quadcopter and the result has validated through MATLAB simulation.[21]

There were many causes contributing in the instability phenomena in quadcopter, such as the ground and wall effects. A study regarding the effects on the stability of the flight of quadcopter in the proximity of walls and ground is conducted. The simulation was done at different translational velocities to fly over an obstacle. At lower speeds, the swirling rotor flows dominate while at the presence of ground effects, it causes an alternating flow patterns between forward and rear rotors. They also conclude that as the speed increases the drag become dominant and highlights that the pitch moment variations near the obstacle can possibly destabilize the quadcopters.[22]

A study also conducted to design and analyse a quadcopter frame to ensure structural integrity and flight stability. They found that at high angular velocities (12,160 RPM), significant airflow velocities between the rotors were produced, which can destabilize the quadcopter. To conclude, they said that to obtain a better flight stability, the body frame should be designed to have control surfaces.[23]

2.5   Summary and research gap

The reviewed literature highlights several key findings which is the importance of the selection of turbulence modelling and the significant effect of the wind to the aerodynamic performance of the quadcopter. Despite the extensive research, there is a need for more studies on the effects of the different angle of incidence of the wind on the stability of the quadcopters. Additionally, the impact of varying angles of incidence on quadcopter and their interaction between the multi-rotor configurations is not well understood. Hence, this current study aims to address this research gap by investigating the aerodynamic performance through varying the angle of incidence of the incoming airspeed. This study will provide valuable insight into optimizing the quadcopter design and performance.

Chapter 3

METHODOLOGY

This section documents the entire of process for the computational fluid dynamics for this study Three primary softwares employed in sequence for this process are Dassault Systèmes SolidWorks, Ansys Fluent and Microsoft Excel. The steps involved are outlined in Figure 3.1.
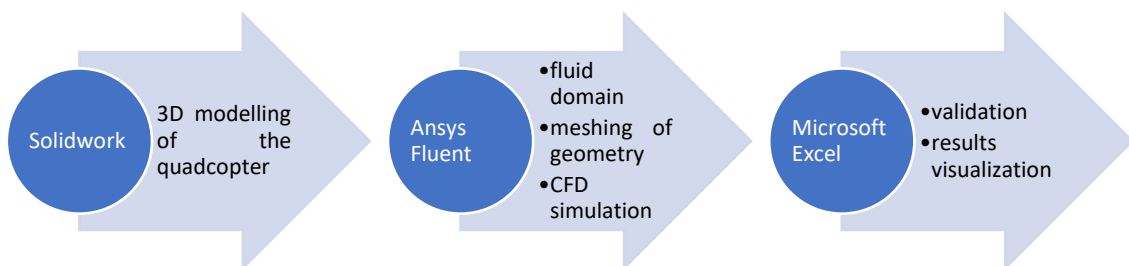
Figure 3.1 : Layout of Processes in the Simulation Study

3.1   3D Modelling of Quadcopter

3.1.1   Quadcopter

In this section, the focus is on the quadcopter used in this study which is DJI phantom 3 (shown in Figure 3.2). DJI Phantom 3 is chosen in this study due to the fact that it is one of the most popular and widely used quadcopters in the market. Due to its popularity, there are many data available for validation of the simulation results which can greatly enhance the credibility and reliability of this study.

Figure 3.2: An image of DJI Phantom 3

3.1.2 CAD Modelling of Quadcopter

The original quadcopter actually consists of camera support assembly and two supporting legs, however to simplify the geometry, the lower part of body has been removed. In solidwork, the fuselage of this quadcopter is firstly offsetting four different planes from the front plane then draw a circle for each of the offset plane then loft it so that a preliminary drone shape is created. Then, fillet is applied to avoid any sharp edges in the geometry to prevent from failure in the meshing phase.

To ensure the geometry is correct, the geometry (Figure 3.3) is then imported into Design Modeller to check if any faces or entities need to be repaired.
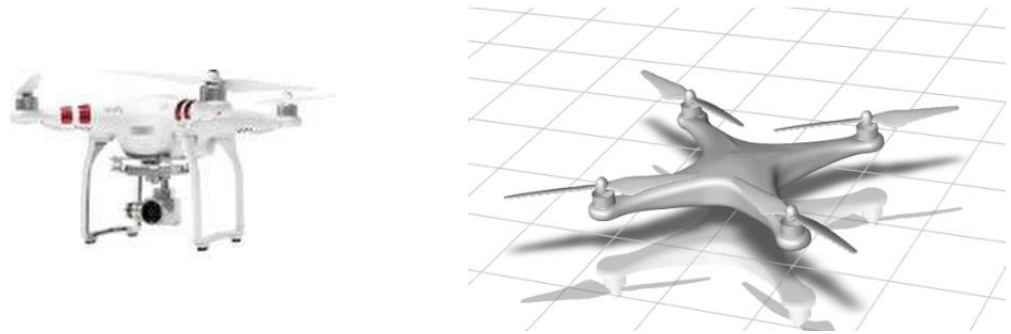

Figure 3.3: Original DJI phantom 3 (left) and simplified DJI phantom 3 used in this study

3.1.3 Propeller

The propeller used in this study is DJI Phantom 9450. This propeller has been experimentally tested for its aerodynamic performance for a range of revolution per minutes. Hence, the thrust coefficient of this propeller can be the benchmark to substantiate the findings.

3.1.4　CAD Modelling of Propeller

The characteristics of the propeller model can be found in Figure 3.4. The figure depicts the width of the chord and twist angle of the propeller blade from the centre of the propeller to the blade tip which also follows the profile of the original propeller geometry of DJI Phantom 9450.

Once the propeller is created, the propeller is then mirrored to another plane such that a counter clockwise propeller and a clockwise propeller are prepared. The geometry parts of the propellers are then assembled to the fuselage of the quadcopter.

To further simplify the meshing process, the propeller is ensured to have no sharp edges and sharp entities.
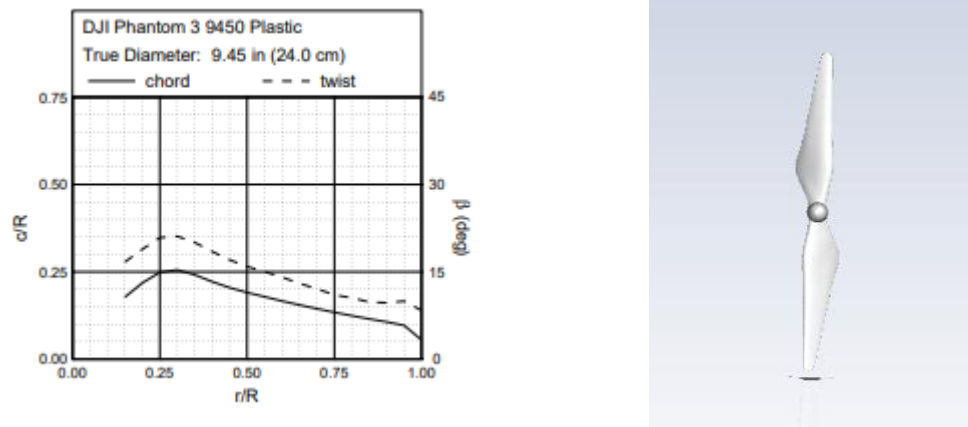
Figure 3.4: Dimension and the Specification of the propeller [5]

3.2　Modelling of Fluid Domain

In this study, the flow field consists of a static and rotating domains. These domains are constructed with Design Modeller which is a package of workbench in Ansys Fluent. 4 smaller cylinder enclosures envelop all the propellers with a diameter of 1.1D and length of 0.2D, which makes up the rotating domain for each of the propellers.

The rotating domain specifications changes with the rotational velocity. The geometry of the rotating domain is illustrated in Figure 3.5 and Figure 3.6.

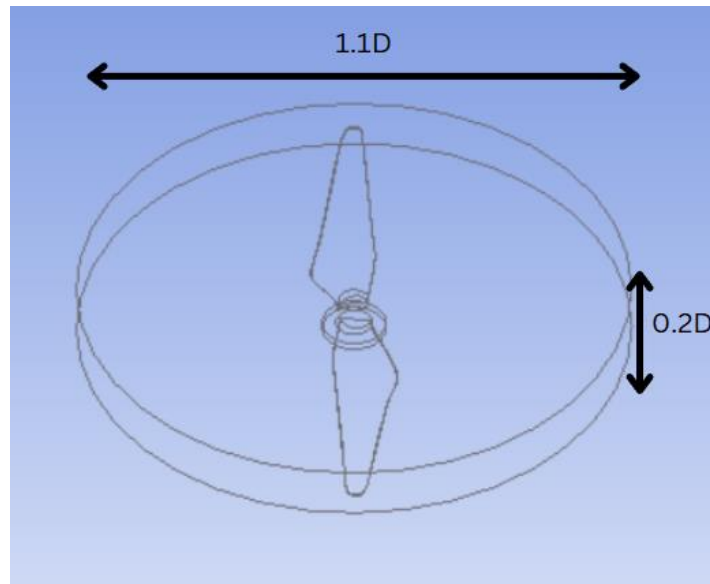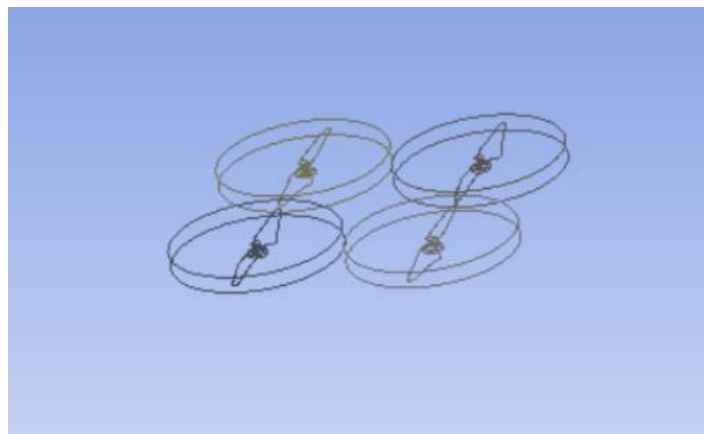Figure 3.5: Geometry of the rotating domain

Figure 3.6: Rotating Domains for All Four Propellers

A static domain is then constructed by creating a cylinder enclosure to envelop the whole quadcopter. The dimension of the static domain is adjusted such that there will be no wall effects and no reverse flow during the simulation. The geometry and the dimension of the static domain is illustrated in Figure 3.7.
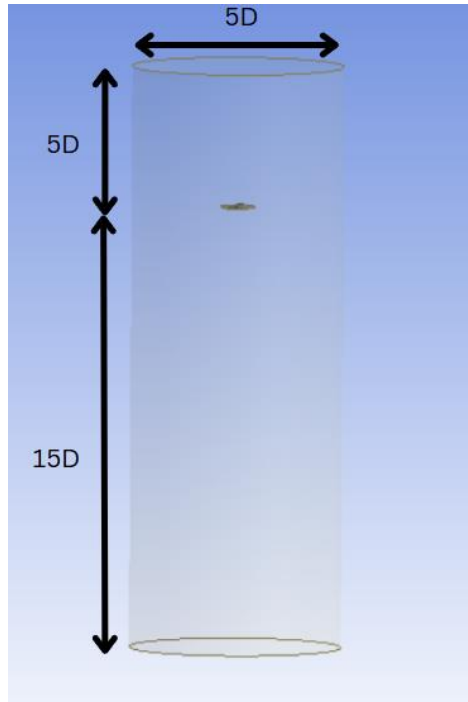
Figure 3.7: Geometry of Static Domain

3.3 Meshing of Geometry

Once the geometry is completed including the flow domain, it is imported into the Mesh workbench for grid generation. The grid generated in this study is poly hex core due to the complex and irregular geometry nature of the propeller. poly hexcore meshes generally means to combine hexahedral and polyhedral cells which give a higher quality meshes compared to purely tetrahedral meshes (which also generally used in complex and irregular geometry) also gives better convergence behaviour at a lower computational cost.

A local refinement is also created around the quadcopter to enhance the accuracy of the results, improved resolution of aerodynamic phenomena and optimized the computational cost. It aims to reduce the numerical errors and captures the complex interactions between propellers and the airframe. Figure 3.8 below shows the mesh of the geometry.
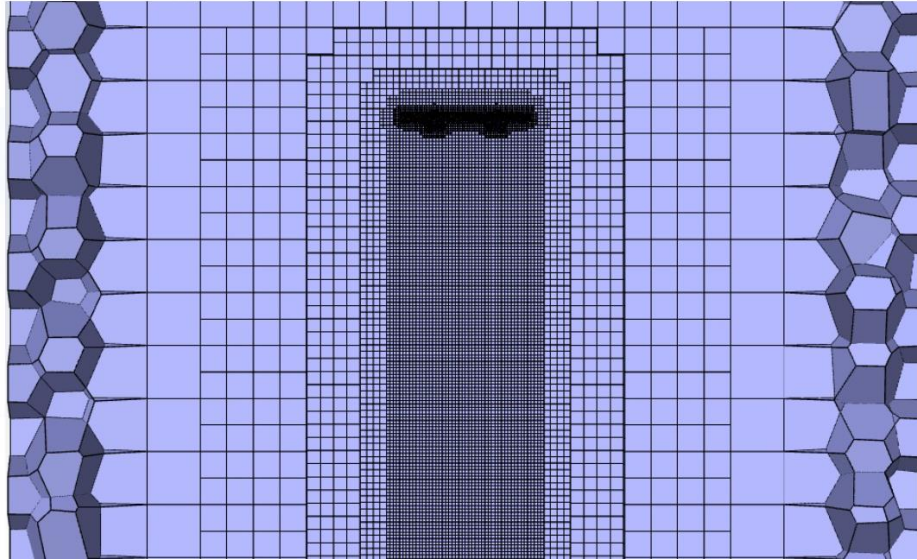
Figure 3.8: Mesh of Rotating and Static Domain

The details of the mesh is shown in Table 3.1

Table 3.1 : Details of the mesh generated

Mesh size type	Number of elements	Maximum skewness	Minimum Orthogonal quality	y^+
coarse	1094921	0.94	0.15	>50
medium	3898408	0.9	0.2	30-50
fine	6293820	0.88	0.2	30-50

For this study the velocity inlet and pressure outlet is defined at the top surface and the bottom surface of the static domain respectively while the surface remained are defined as symmetry to simulate a hovering quadcopter in open air and to model a zero shear-slip wall for the airflow. The detailed positioning of the inlet, outlet and symmetry are shown in Figure 3.9.
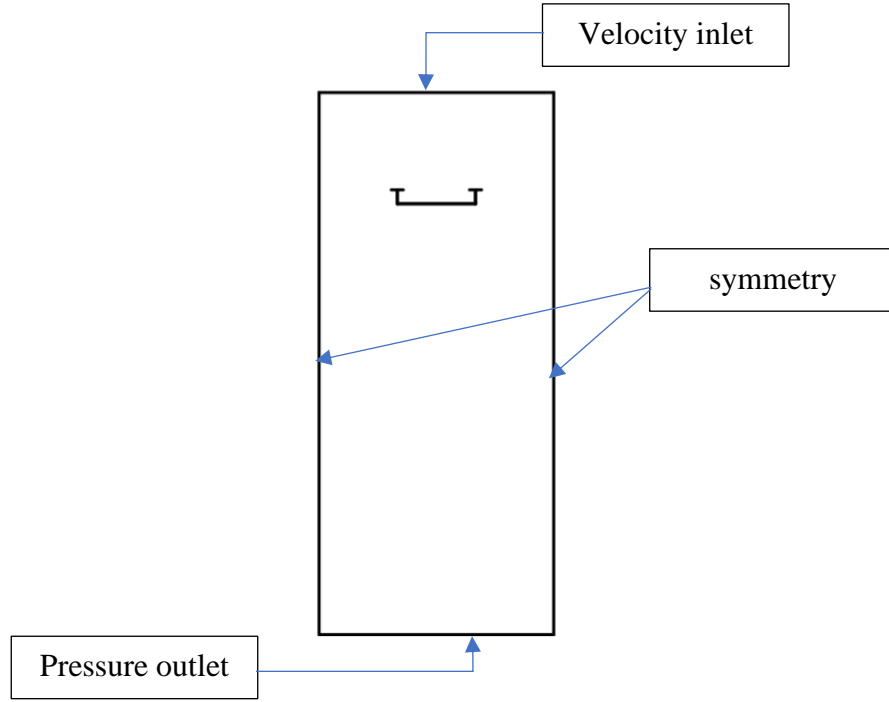
Figure 3.9: Positioning of the Velocity Inlet, Pressure Inlet and Symmetry

3.4   Computational Fluid Dynamics Simulation

Pressure-based transient simulation is conducted in this study. The numerical model employed for this study for computational fluid dynamics simulation is the standard k-epsilon model. Due to the time and computational power constraint, only two-equation models are considered.

The governing equation of the fluid flow are the Navier-Stokes equations and is solved through the incompressible Reynolds-Averaged Navier-Stokes (RANS) equations

Conservation of mass, in Einstein notation:

$$\frac{\partial U_i}{\partial x_i} = 0 \qquad (3.1)$$

Where U_i represents the i-th component of the velocity vector and x_i represents the i-th spatial coordinate. The repeated index i implies the summation over all spatial dimensions, hence it is expanded into:

$$\frac{\partial U_1}{\partial x_1} + \frac{\partial U_2}{\partial x_2} + \frac{\partial U_3}{\partial x_3} = 0 \qquad (3.2)$$

This equation signifies that the divergence of the velocity field is zero, ensuring that the fluid density remains constant and that there is no net flow out of any infinitesimal volume within the fluid. This is a fundamental condition for incompressible flow, indicating that the volume of fluid elements remains unchanged as they move through the flow field.

RANS :

Reynolds-stress

$$\rho \frac{\partial U}{\partial t} + \rho \nabla \cdot (UU) = -\nabla p + \nabla \cdot [\mu(\nabla U + (\nabla U)^T)] + \rho g - \nabla\left(\frac{2}{3}\mu(\nabla \cdot U)\right) - \rho \nabla \cdot (\overline{U'U'}) \qquad (3.3)$$

Where,

ρ = density of the fluid

μ = dynamic viscosity of the fluid

U = the time-averaged component of velocity

$U^{'}$ = the fluctuating component of velocity

The standard k-epsilon model is chosen for its properties to accurately capture the effects of turbulence on flow characteristics. It can solve two transport equations which is the turbulent kinetic energy (k) and one for the turbulent dissipation rate (ϵ) which can be expressed as below.[8]

Transport equation for k :

$$\rho \frac{\partial k}{\partial t} + \rho \nabla \cdot (Uk) = \nabla \cdot \left[\left(\mu + \frac{\mu_t}{\sigma_k}\right)\nabla k\right] + P_k + P_b - \rho\epsilon \qquad (3.4)$$

24

Transport equation for ϵ :

$$\rho\frac{\partial\epsilon}{\partial t} + \rho\nabla\cdot(U\epsilon) = \nabla\cdot\left[\left(\mu+\frac{\mu_t}{\sigma_\epsilon}\right)\nabla\epsilon\right] + C_1\frac{\epsilon}{k}(P_k + C_3P_b) - C_2\rho\frac{\epsilon^2}{k} \qquad (3.5)$$

The standard k-epsilon model with enhanced wall treatment are used to fix the problem of divergence as it can accurately model the flow near solid boundaries even with relatively coarse meshes that do not resolve the viscous sublayer ($y^+ > 30$).

To simulate the rotating flow of the rotor, the rotating domain was simulated as a sliding mesh model by activating mesh motion in its cell zone conditions. Mesh motion moves the rotating domain as per the rpm specified. Mesh motion is suitable for predicting flow transfer across interface without any sort of averaging such as transfer of eddies.

As for the time step size, the simulation will be initially run at a bigger time step size and then the time step size is then altered with a smaller time step size once a converged result is obtained. The purpose of using a larger time step size in the early stage is to accelerate the convergence process. This initial phase aimed to quickly bring the simulation closer to a steady or quasi-steady state, allowing for a rough approximation of the flow field. As the simulation approached convergence, the time step size was reduced to capture more detailed and accurate flow characteristics. This refinement was essential for resolving transient phenomena and fine-scale features of the flow. The smaller time step size is calculated using the equation below (at courant number equals to one).

$$dt = \frac{m}{\pi D n} \qquad (3.6)$$

Where,

dt = time step size

m = mesh size of the rotating domain (mm)

D= diameter of the rotating domain (mm)

n = rotating velocity (revolution per second)

In summary, Table 3.2 shows the summary of the setup of the simulation

Table 3.2: Setup of the Simulation

Solver	Pressure-based
Time state	transient
Turbulent model	k-epsilon
Wall function	Near-wall treatment
Flow fluid	air
Inlet velocity	3 m/s
Method	Coupled pressure-velocity scheme
No. Iteration per time step	200 (0.1s) then 400 (based on the Equation)

3.6   Validation

The thrust force obtained from the simulation in Ansys Fluent was converted to thrust coefficient and compared against the experimental thrust coefficient. The plot of experimental thrust coefficient is shown in Figure 3.10. The thrust coefficient was computed using Equation (2.2) stated in the literature review.
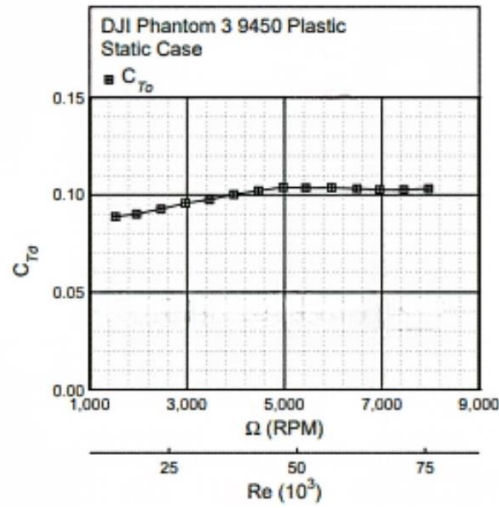
Figure 3.10: Thrust Coefficient against RPM from Experimental Data

3.5   Varying velocity angle at the velocity inlet

A range of inlet angles are chosen in this study. An increment of $10°$ from $0°$ to $40°$ are applied in this study to represent different flight conditions and environmental scenarios. For each of the inlet angle, all the constants are remain constant, with the incoming airflow velocity of 3 m/s and the aerodynamic performance such as the thrust force is then extract from the simulation. By visualizing the flow with the contours, the results are compared across different inlet angles to identify trends and variations in performance. Figure 3.11 below shows a schematic diagram of the scenarios.
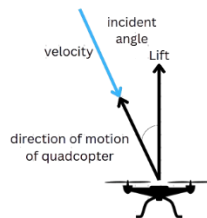

Figure 3.11: Schematic diagram of the Intended Simulation

28

Chapter 4

RESULT AND DISCUSSION

4.1 Grid Independence Test

In computational fluid dynamics simulation, the accuracy of the simulation results is highly dependent on the quality of the computational mesh. Grid independence test is needed to ensure the appropriate number of mesh size for an accurate enough result. In this study, the accuracy of the results is compared with the thrust coefficients obtained from the experimental results.

Three different mesh densities from coarse to fine has been conducted as in Table 4.. The coarse mesh represents the lowest resolution which consists of 1094921 nodes, the medium mesh represents an intermediate resolution which consists of 3898408 nodes while the fine mesh represents a higher resolution which consists of 6293820 nodes. From Table 4. and Figure 4.1, it can be seen that the thrust coefficient does not deviates much. However, the error between the experimental thrust coefficient and numerical thrust coefficient are decreasing as the number of nodes of the mesh is increasing. As the accuracy is improving the drawback is getting more obvious which is the a higher computational cost are required to run the simulation at a finer mesh.

Ultimately, this grid independence test demonstrates that the accuracy of the simulation results improves with increasing mesh density. As can be seen in Table 4. and Figure 4.1, the medium mesh density (3898408 nodes) gives a good balance between the accuracy and computational cost, as the results have sufficiently converged, showing that they are independent of further mesh refinement. As a result, the medium mesh will used

for the subsequent simulation in this study to ensure a reliable and an accurate result without wasting much computational cost.

Table 4.1: Grid independence test results

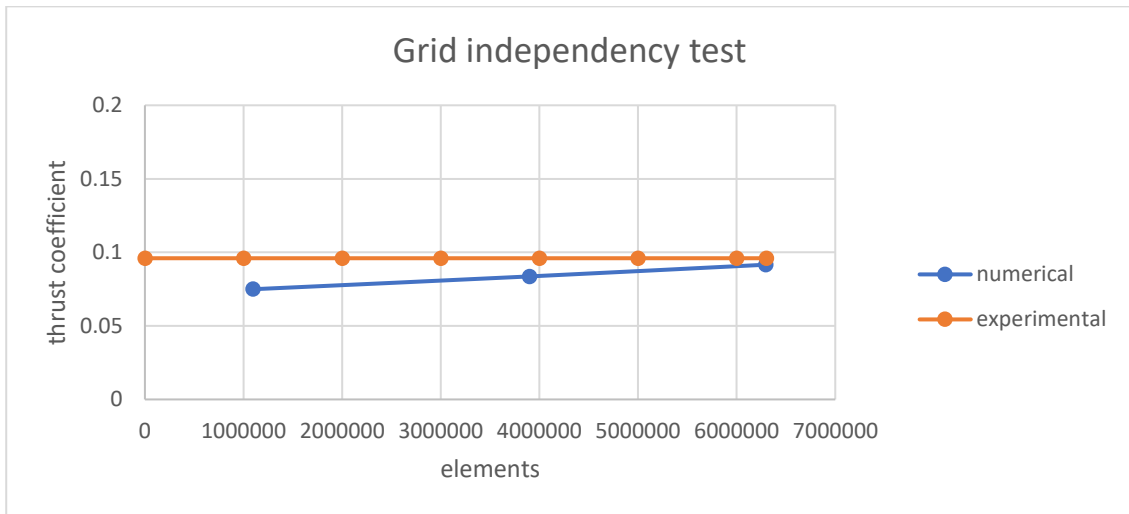| nodes	Experimental thrust coefficient [5]	Numerical thrust coefficient	error	difference from the previous mesh (%)	time taken
1094921		0.074931678	0.21946169	-	4-5 hours
3898408	0.096	0.083626622	0.12888935	11.60382929	10+ hours
6293820		0.091598561	0.04584833	9.532776536	more than 2 days

Figure 4.1: Graph Visualization of the Grid Independency Test Results.

4.3 Aerodynamic Performance

Validation of the propellers of the quadcopter with the experimental data is conducted and can be seen in Table 4. and Figure 4.2. As can be seen in Table 4., the thrust coefficient computed numerically is fairly close to the experimental results, with

an error of a range of 11% to 15%. Since the error is considerably small, it can be said

that the results are considerably accurate.

Table 4.2: Validation Results of Numerical Thrust Coefficient to the Experimental
Thrust Coefficient.

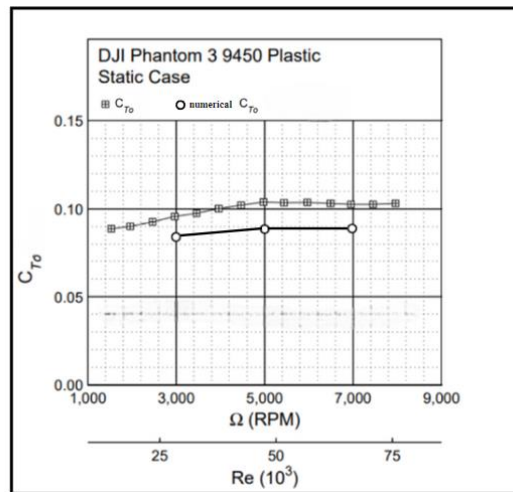| rpm	experimental thrust coefficient [5]	numerical thrust coefficient	error (%)
3000 rpm	0.095	0.083626622	11.97198
5000rpm	0.103	0.087726757	14.82839
7000 rpm	0.102	0.088740658	12.99936

Figure 4.2: Graph Visualization of the Validation Results of Numerical Thrust
Coefficient to the Experimental Thrust Coefficient.

4.4   Varying angle of incidence of the velocity at velocity inlet

In this section, the aerodynamic performance of the quadcopter subjected to

varying angles of incident velocity ranging from 0° to 40° is discussed. With the help

with the quantitative lift and thrust data and the pressure contours of the quadcopter

aimed to offer a comprehensive understanding of the quadcopter's behaviour.

The velocity contour of this study is compared to the work of Weerasinghe.

S.R.[19] in Figure 4.3. The velocity contour of this study at 10° (Figure 4.3left) is

compared to the velocity contour of Weerasinghe study (Figure 4.3 right). It is shown that the pattern of the flow is quite similar which gives some credibility to the current study.
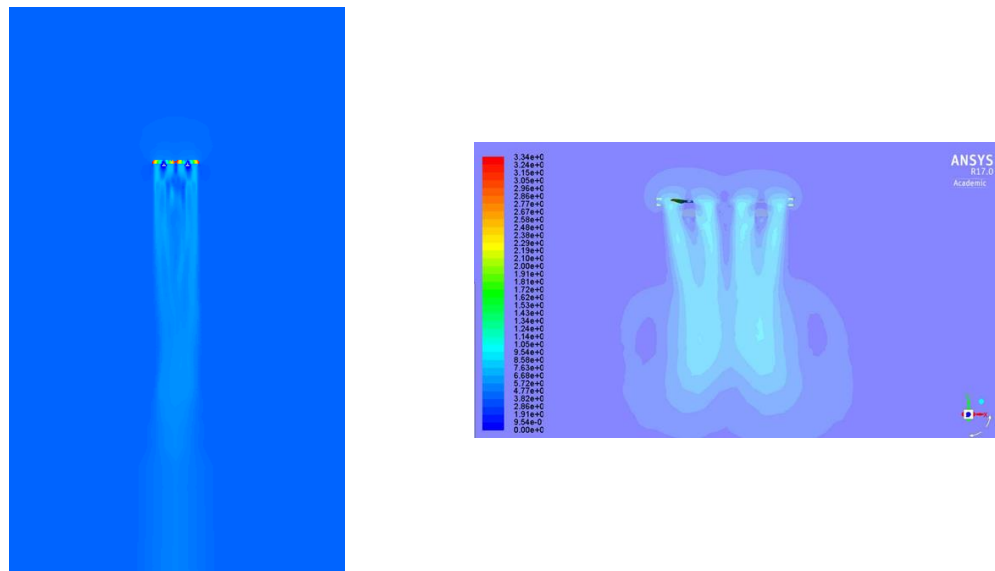

Figure 4.3: Comparative study between (A) current study at 10° and (B) Weerasinghe's study

Figure 4.4 shows the static performance and the dynamic performance. As can be seen in Figure 4.4, the thrust coefficient remains constant without airflow across all angles but deteriorates greatly with airflow as the angle increases. This contrast highlights the importance of real world airflow considerations in performance evaluation because static tests alone do not capture the full picture of the aerodynamic performance of the quadcopter.

Table 4. shows the quantitative data of the aerodynamic performance trends across different incident velocity angles. As seen from Table 4., the lift response to the angle changes is quite minimal although a peak at the lift force of the quadcopter observed at 20°. However, it can be seen that the thrust of the quadcopter depicts a trend of declination with the increasing angle. Since the introduction of the incoming airflow

velocity with 3m/s from the velocity inlet, the thrust coefficients have been deteriorated 20% to 40% from the initial numerical thrust coefficient across the varying angles of incident velocity. This declination indicates the aerodynamic challenges at higher angles where maintaining enough thrust has become increasingly adverse. Since the lift generated across the varying angles can be considerably constant, it can be said that the lift to thrust ratio is also decreasing. This suggest that while lift can be somewhat maintained, thrust efficiency deteriorates significantly with increasing angles.

Figure 4.5 shows the pressure contour of the quadcopter. This pressure contour visualizations show the significant aerodynamic changes as the incident velocity angle increases. As can be seen in Figure 4.5, at lower angle which is ranging from 0° to 20°, the pressure distribution exhibits a relatively symmetry nature which can be indicating that the aerodynamic performance is quite stable. As the angle increases to 30° and 40°, it can be seen that a significant asymmetry emerges in the pressure distribution. This transition suggests a potential instability that could adversely affect the overall stability and control of the quadcopter. The asymmetry of the pressure contour can also explain the decrease in thrust coefficient as the angle increases.

Table 4.3: Aerodynamic Performance at Rotational Speed of 3000 RPM at Varying Velocity Inlet Angles

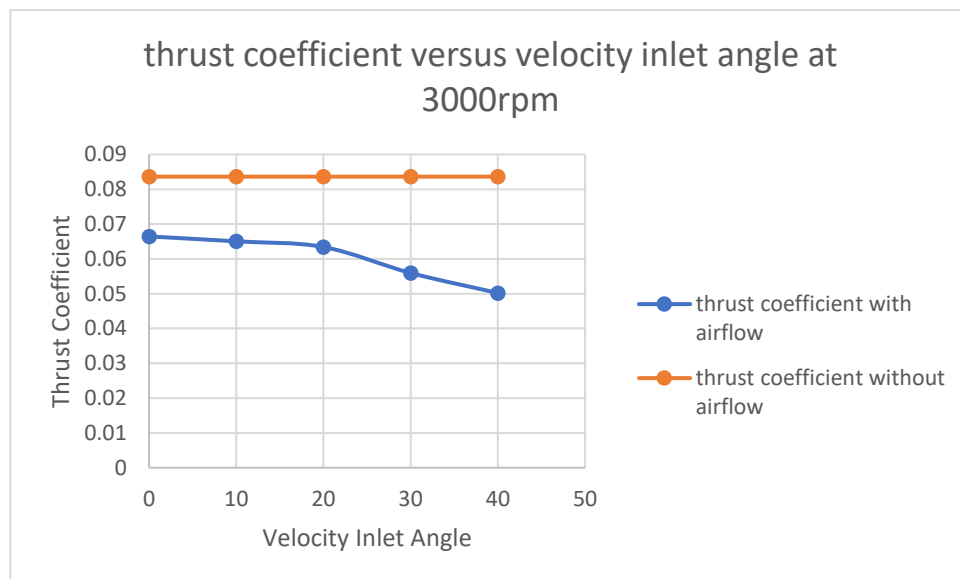| Rotational speed	Velocity inlet angles	Lift generated	Thrust coefficient
3000 rpm	$0°$	0.675144	0.066447005
	$10°$	0.670952	0.065039812
	$20°$	0.685994	0.063411734
	$30°$	0.657905	0.055950003
	$40°$	0.667643	0.050199821

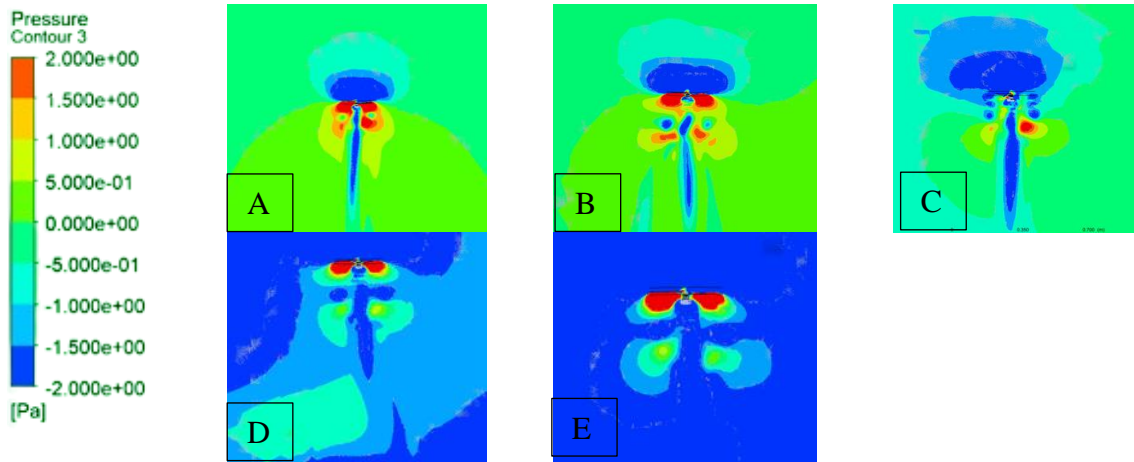Figure 4.4: Graph of Thrust Coefficient Versus Velocity Inlet Angles at 3000 RPM

Figure 4.5: Pressure contour of one of the propeller at (A) 0° (B) 10°(C) 20°(D) 30° (E) 40° angle of incident of the velocity from inlet.

The progression of vortex structures of instantaneous Q-criterion from 0 to 40 degrees in Figure 4.6 reveals a complex evolution of the quadcopter's aerodynamics. At 0 degrees, symmetrical, elongated vortices trailing from each rotor are observed, indicative of a stable hover condition. As the angle increases, asymmetry becomes increasingly pronounced. By 10 degrees, vortices begin to bend, with forward rotor vortices shortening and rear ones elongating. This trend intensifies at 20 degrees, where the asymmetry becomes more evident. At 30 degrees, a drastic change with highly disrupted forward rotor vortices and sharply curved rear vortices is observed, suggesting significant flow separation and potential loss of lift on the forward rotors. The 40-degree angle presents an extreme case, with almost non-existent forward rotor vortices and excessively elongated, curved rear vortices, indicating severe flow disturbance and likely substantial control challenges. This progression demonstrates the transition from a stable hover to increasingly complex and potentially unstable forward flight conditions. The changes in vortex length, curvature, and interaction provide insights into shifting lift distribution, control requirements, and overall vehicle stability. The shortening of forward rotor vortices suggests reduced efficiency and potential loss of lift, while the elongation and curvature of rear rotor vortices indicate increased workload on these rotors to maintain

35

lift and control. The increasing asymmetry and vortex interactions at higher angles point to greater aerodynamic complexity, likely necessitating more sophisticated control strategies to maintain stable flight.
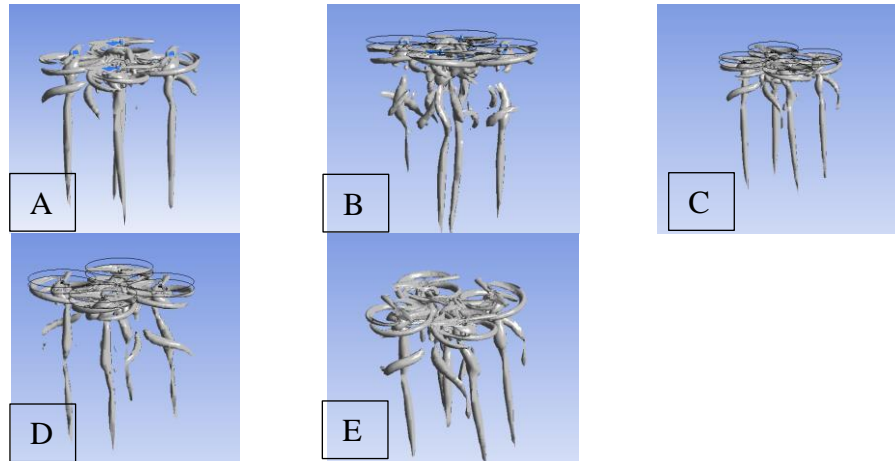
Figure 4.6: vorticity core of Q criterion at $2572.02s^{-2}$ at (A) 0° (B) 10°(C) 20°(D) 30° (E) 40° angle of incident of the velocity from inlet.

The study also further explore at a rotational speed of 7000 RPM, which shows that at 0° and 10° the pressure contour (shown in Figure 4.7) has already shown asymmetry pattern. Hence it is safe to say that the quadcopter will experience instability at a smaller velocity angle as the rotational speed increases.

Figure 4.7: Pressure contour of one propeller at 0° (left) and 10°(right) velocity angle

Chapter 5

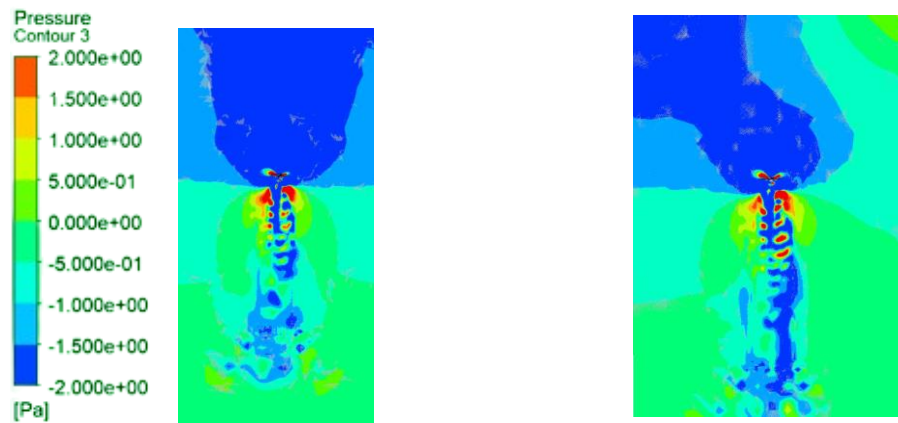## CONCLUSION AND RECOMMENDATION

5.1   Conclusion

This study has provided a detailed investigation into the aerodynamic performance of quadcopter under varying angles of incident velocity ranging from 0° to 40° at a rotational speed of 3000 rpm and 7000 rpm.

The analysis revealed a clear relationship between the inlet angles and thrust production. As the inlet angle increased, thrust consistently decreased. Throughout all the various inlet angles, the thrust coefficient has deteriorated 20-40%. This finding highlights the critical impact of inlet angles on the quadcopter's aerodynamic performance particularly on the thrust capabilities.

Peak efficiency was observed in the range of 0° to 20°, with the thrust coefficient remaining relatively stable in this range. However, efficiency degraded rapidly at higher angles, particularly beyond 30°. The pressure contour and vorticity visualizations corroborated these findings, showing balanced pressure distributions at lower angles transitioning to disrupted patterns at higher angles. These results underscore the importance of maintaining lower inlet angles and at low rotational speed to preserve aerodynamic efficiency in quadcopter operations.

At lower angles (0° to 20°), the flow remained largely stable with minimal separation. However, as angles increased to 30° and 40°, significant flow instabilities were observed. These manifested as large low-pressure zones, asymmetrical pressure distributions, and evidence of flow separation. The wake region also showed increased turbulence at higher angles, indicating potential interference issues in multi-rotor

configurations. These observations of flow instability directly correlate with the decreased thrust and efficiency at higher angles.

At 7000 rpm, the instability is becoming profound in smaller inlet angle. It is seen that at 0° already shown some instability but still consider stable however at 10°, the asymmetry feature in the pressure contour has revealed that it is hard to achieve stable. These observations can be concluded that at higher rotational speed, the instability become more profound at smaller inlet angle.

In conclusion, The findings clearly indicate that maintaining inlet angles below 20° at 3000 rpm is crucial for optimal quadcopter performance, balancing thrust production, aerodynamic efficiency, and flow stability. These results provide valuable guidance for quadcopter design and operation, enabling more informed decision-making to enhance performance across diverse flight conditions.

5.2 Recommendations for Future Research

Based on this research, following are several recommendations for future research. Future work should focus on investigating finer angle increments, especially in the critical 0° to 30° range. Besides that, an angle range between 0° to 10° at 7000 rpm can be analysed in the future to have a better picture on how the instability occur. Also, future work also can be done on developing an adaptive propeller designs or control systems to optimize the performance across the diverse flight conditions.

REFERENCES

[1]   D. S. Pachpute, "Working Principle and Components of Drone · CFD Flow Engineering," 2020.

[2]   S. Yoon, H. C. Lee, and T. H. Pulliam, "Computational analysis of multi-rotor flows," in *54th AIAA Aerospace Sciences Meeting*, 2016. doi: 10.2514/6.2016-0812.

[3]   S. Gudmundsson, *General Aviation Aircraft Design: Applied Methods and Procedures*. 2022. doi: 10.1016/B978-0-12-818465-3.09989-4.

[4]   B. W. McCormick, "Aerodynamics Aeronautics and Flight Mechanics John Wiley & Sons.," *Inc., New York*, 1979.

[5]   R. W. Deters, S. Kleinke, and M. S. Selig, "Static testing of propulsion elements for small multirotor unmanned aerial vehicles," in *35th AIAA Applied Aerodynamics Conference, 2017*, 2017. doi: 10.2514/6.2017-3743.

[6]   I. Penkov and D. Aleksandrov, "Propeller shrouding influence on lift force of mini unmanned quadcopter," *International Journal of Automotive and Mechanical Engineering*, vol. 14, no. 3, 2017, doi: 10.15282/ijame.14.3.2017.7.0354.

[7]   Y. Gu *et al.*, "Numerical and experimental studies on the owl-inspired propellers with various serrated trailing edges," *Applied Acoustics*, vol. 220, 2024, doi: 10.1016/j.apacoust.2024.109948.

[8]   W. P. Jones and B. E. Launder, "The prediction of laminarization with a two-equation model of turbulence," *Int J Heat Mass Transf*, vol. 15, no. 2, 1972, doi: 10.1016/0017-9310(72)90076-2.

[9]   A. Sapit, M. F. Masjan, and S. K. Shater, "Aerodynamics Drone Propeller Analysis by using Computational Fluid Dynamics," *Journal of Complex Flow*, vol. 3, no. 2, pp. 12–16, 2021, [Online]. Available: https://fazpublishing.com/jcf/index.php/jcf/article/view/35

[10]   P. R. Spalart and S. R. Allmaras, "One-equation turbulence model for aerodynamic flows," *Recherche aerospatiale*, no. 1, 1994, doi: 10.2514/6.1992-439.

[11]   Č. Kostić, "Review of the Spalart-Allmaras turbulence model and its modifications to three-dimensional supersonic configurations," *Scientific Technical Review*, vol. 65, no. 1, 2016, doi: 10.5937/str1501043k.

[12]   D. Adanta, I. M. R. Fattah, and N. M. Muhammad, "COMPARISON OF STANDARD k-epsilon AND SST k-omega TURBULENCE MODEL FOR BREASTSHOT WATERWHEEL SIMULATION," *Journal of Mechanical Science and Engineering*, vol. 7, no. 2, 2020, doi: 10.36706/jmse.v7i2.44.

[13]   A. M. Pérez G., O. D. López, and J. A. Escobar, "Computational study of the wake of a quadcopter propeller in hover," in *23rd AIAA Computational Fluid Dynamics Conference, 2017*, 2017. doi: 10.2514/6.2017-3961.

[14]   S. H. Almallah, A. O. Elnady, and A. Okasha Elnady, "CFD Analysis of Full Quadcopter," *International Journal of Advanced Multidisciplinary Research and Studies*, vol. 2, no. December 2022, 2023.

[15]   A. J. Fultz and W. S. Ashley, "Fatal weather-related general aviation accidents in the United States," *Phys Geogr*, vol. 37, no. 5, 2016, doi: 10.1080/02723646.2016.1211854.

[16]   W. Knecht and M. Lenz, "Causes of General Aviation Weather-Related, Non-Fatal Incidents: Analysis Using NASA Aviation Safety Reporting System Data," p. 52, Sep. 2010.

[17]   G. Capobianco and M. D. Lee, "The role of weather in general aviation accidents: An analysis of causes, contributing factors and issues," in *Proceedings of the Human Factors and Ergonomics Society*, 2001. doi: 10.1177/154193120104500241.

[18]   M. MURAKAMI, H. ABE, H. AONO, and H. ISHIKAWA, "Effects of gusty flow on aerodynamic performance of multirotor drone propellers in hovering flight," *Journal of Fluid Science and Technology*, vol. 17, no. 4, 2022, doi: 10.1299/jfst.2022jfst0013.

[19]   Weerasinghe SR and Monasor M, "Simulation and Experimental Analysis of Hovering and Flight of a Quadrotor," *13th International Conference on Heat Transfer, Fluid Mechanics and Thermodynamics*, 2017.

[20]   Y. Lei and M. Cheng, "Aerodynamic performance of Hex-Rotor UAV considering the horizontal airflow," *Applied Sciences (Switzerland)*, vol. 9, no. 22, 2019, doi: 10.3390/app9224797.

[21]   V. Praveen and A. S. Pillai, "Modeling and simulation of quadcopter using PID controller," *International Journal of Control Theory and Applications*, vol. 9, no. 15, 2016.

[22]   C. Paz, E. Suárez, C. Gil, and C. Baker, "CFD analysis of the aerodynamic effects on the stability of the flight of a quadcopter UAV in the proximity of walls and

ground," *Journal of Wind Engineering and Industrial Aerodynamics*, vol. 206, 2020, doi: 10.1016/j.jweia.2020.104378.

[23] E. Kuantama, D. Craciun, and R. Tarca, "QUADCOPTER BODY FRAME MODEL AND ANALYSIS," *ANNALS OF THE ORADEA UNIVERSITY. Fascicle of Management and Technological Engineering.*, vol. Volume XXV, May 2016, doi: 10.15660/AUOFMTE.2016-1.3205.